JOURNAL OF MATERIALS SCIENCE 31 (1996) 565–571

The effect of Ti-colloid surface conditioning on the phosphating of 7075-T6 aluminium alloy

J. F. YING, M. Y. ZHOU, B. J. FLINN, P. C. WONG, K. A. R. MITCHELL
Department of Chemistry, University of British Columbia, 2036 Main Mall, Vancouver British Columbia, Canada, V6T 1Z1

T. FOSTER
Chemistry Group, Defence Research Establishment Pacific, FMO Victoria, British Columbia, Canada, V0S 1B0

7075-T6 aluminium alloys panels were surface conditioned in a titanium colloid suspension, under a variety of different conditions, and subsequently these samples were immersed in a $ZnO + H_3PO_4$ coating mixture, and the phosphate coating layers characterized. Morphologies observed by scanning electron microscopy (SEM) reveal that the coating layer consists of two phases, namely an amorphous phase, which is directly bonded to the substrate, and a crystalline phase, in which larger crystal grains grow on top of the amorphous base. Chemical compositions of the coating layers were analysed by X-ray photoelectron spectroscopy (XPS) and by static and imaging secondary ion mass spectroscopy (SIMS). It is found that the details of the surface conditioning affect the final coating, both in terms of morphology and chemical composition. For example, larger amounts of Zn and P are detected in coatings for which the initial conditioning is done at 40 °C, compared with room temperature; a similar statement can be made for surfaces which are water rinsed after the Ti pretreatment, compared with those which are not water rinsed prior to the coating treatment.

1. Introduction

Corrosion protection of aluminium is of great importance due to its widespread usage by various industries, especially in aerospace industries. Conventionally for aluminium alloys, zinc chromate has been used as a pigment in anticorrosive primers, as well as being used in conversion coating and anodizing processes. However, industrial usage of zinc chromate is being increasingly restricted due to its toxicity and the resulting environmental impact. One of the possible replacements for zinc chromate pigments and the zinc chromate surface treatment that has been considered is zinc phosphate, which is an established anticorrosion pigment and treatment process for steel [1–3].

Rausch [4] has summarized the coating chemistries of phosphating processes on steel, including the effects of various additives, the morphologies and the corrosion resistance properties. In comparison, knowledge about zinc phosphate coatings on aluminium is much less comprehensive. In the phosphating of steel, the properties of phosphate coatings can be influenced by prerinsing with Ti solutions and adding components, e.g. fluoride, to the coating bath, and similar effects have also been investigated in studies on the phosphating of aluminium [5–8]. Recently, various zinc phosphating processes on 7075-T6 aluminium alloy have been studied [9–11] with emphasis on the effects of different pH levels and fluoride additives in the coating bath, and the surfaces characterized both by morphology observation and by XPS. Information on the chemical state/composition of the coating layer has shed new light on the coating chemistry of the zinc phosphating processes. Among the coating baths investigated, $ZnO + H_3PO_4$ suspensions at elevated temperatures appear to produce higher levels of zinc phosphate in the coating layers, which turn out to have mixed composition, i.e. $Zn_xAl_yPO_4$ [9–11]. Furthermore, fluoride additive to the coating bath has the general effect of enhancing Zn and P content in the coating layer, which is consistent with the earlier study by Turuno *et al.* [7].

The present work focuses on studying the effects of Ti colloid surface conditioning and the related coating chemistry. As well, the authors aim to improve the phosphating processes based on the $ZnO + H_3PO_4$ coating bath as part of a systematic effort to achieve an optimum zinc phosphate (ZPO) coating on aluminium. A Ti colloid surface conditioning step was included before phosphating, and its effect on the resultant coatings investigated. Different treatment conditions were explored and evaluated based on characterization of the final coating layers with the complementary techniques of SEM, XPS and SIMS. Such an approach should help identify relationships between morphology and chemical state/composition,

0022–2461

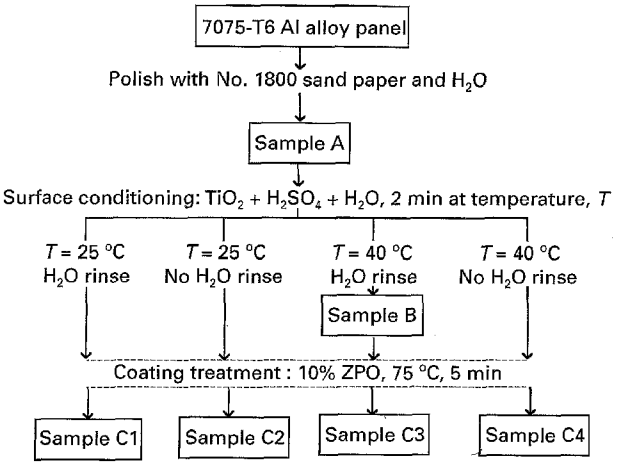

Figure 1 Experimental procedures for Ti colloid conditioning and zinc phosphate coating treatments. Samples from different steps in this work are labelled as A, B, C1, C2, C3 and C4.

and in turn provide both a more effective evaluation for the final coating layer and an improved understanding of the coating chemistry involved.

2. Experimental procedure

Experiments were conducted on square sample panels of 7075-T6 aluminium alloy with dimensions $1 \times 1 \times 0.12$ cm. Procedures for preparing the sample panels have been detailed previously [9]. Briefly, all sample panels were polished with sandpaper and water, and then degreased with acetone and methanol in an ultrasonic bath. The Ti colloid for surface conditioning was prepared with TiO_2, concentrated H_2SO_4 and deionized water, and the surface conditioning was done by immersing the sample panels in the colloidal suspension for 2 min. In the search for optimum conditions, this procedure was carried out both at room temperature and at 40 °C, and with and without subsequent rinsing in distilled water. Sample panels after surface conditioning were treated in the $ZnO + H_3PO_4$ coating suspension for 5 min at 75 °C, followed by rinsing with deionized water and air drying. The above coating procedures are summarized in Fig. 1, where samples from different treatment steps are subsequently used for SEM, XPS and SIMS studies.

Scanning electron micrographs were taken on a Hitachi S4100 SEM using a beam energy of 30 keV, and SIMS analyses were carried out using a VG MM12-12S quadrupole spectrometer with a Ga ion gun (minimum beam size ~0.5 μm). XPS spectra were measured in a Leybold MAX200 spectrometer at an operating pressure of 6×10^{-7} Pa. The unmonochromatized AlK_α source (1486.6 eV) was operated at 15 kV, 20 mA, and the emitted photoelectrons were collected from a 2×4 mm^2 area. Spectra were recorded with the analyser pass energy set at 192 eV. Peak areas for Zn2$p_{3/2}$, P2p and Al2s, determined after background subtraction, were taken to indicate relative elemental amounts after correcting with the appropriate sensitivity factors provided by the manufacturer.

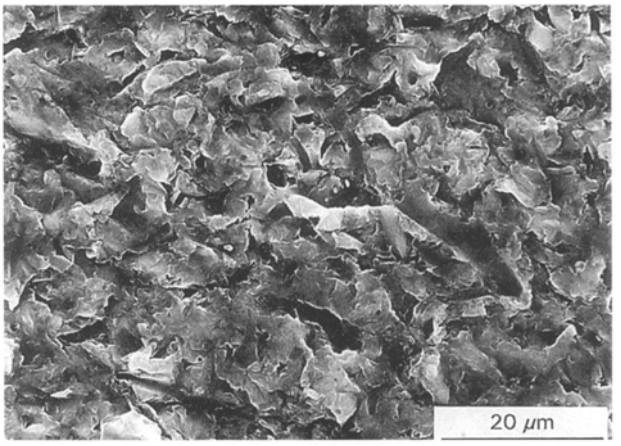

Figure 2 Scanning electron micrograph at ×1500 magnification from sample A (blank Al panel after wet polishing with sandpaper). The field of view is approximately 75 × 60 μm.

3. Results

3.1. Morphologies from SEM

Scanning electron micrographs were taken for samples selected from different steps of the coating process, namely sample A, sample B and samples C1–C4 labelled in Fig. 1. The surface of a blank sample after wet polishing (sample A) has a rough, dark appearance to the eye. The micrograph of sample A at ×1500 magnification is shown in Fig. 2. The polished surface appears quite rough with typical features of dimension ~1–5 μm. Previous studies have shown that the degree of roughness of the initial surface can affect significantly the formation of the coating layer [4]. Among the polishing procedures tested, the present wet polishing procedure, with the corresponding roughness, yielded the best zinc phosphate coatings.

Although the same polishing and coating procedures were done for samples C1–C4, different surface conditioning procedures were applied. Micrographs for the coating layers on these samples are shown in Fig. 3. In general, two phases are apparent for all four samples C1–C4, namely an amorphous coating phase, i.e. the base phase, and the crystalline coating phase, i.e. the crystalline grains on top of the base phase. The amorphous phases appear porous with dense microscopic hole structures, a constant feature for samples C1–C4, i.e. the amorphous base phase seems to be largely unaffected by the different surface conditioning procedures. These phases have been checked with the highest magnification available 300 000; they appear to be homogeneous, with no evidence of finer grain structure down to the 10 nm scale. Fig. 4 shows a micrograph at ×15 000 magnification for sample C4 to give a closer examination of the crystal grains. These grains appear to grow, rather than be physically trapped, on the amorphous base phase. Furthermore, the size, density and distribution of the crystal grains are clearly affected by the different surface conditioning procedures according to the micrographs in Fig. 3. For samples C1 and C2, that were surface conditioned at room temperature, the crystal grains are scattered and separated with a relatively large size (~5 μm). On the other hand, patches of crystal clusters were

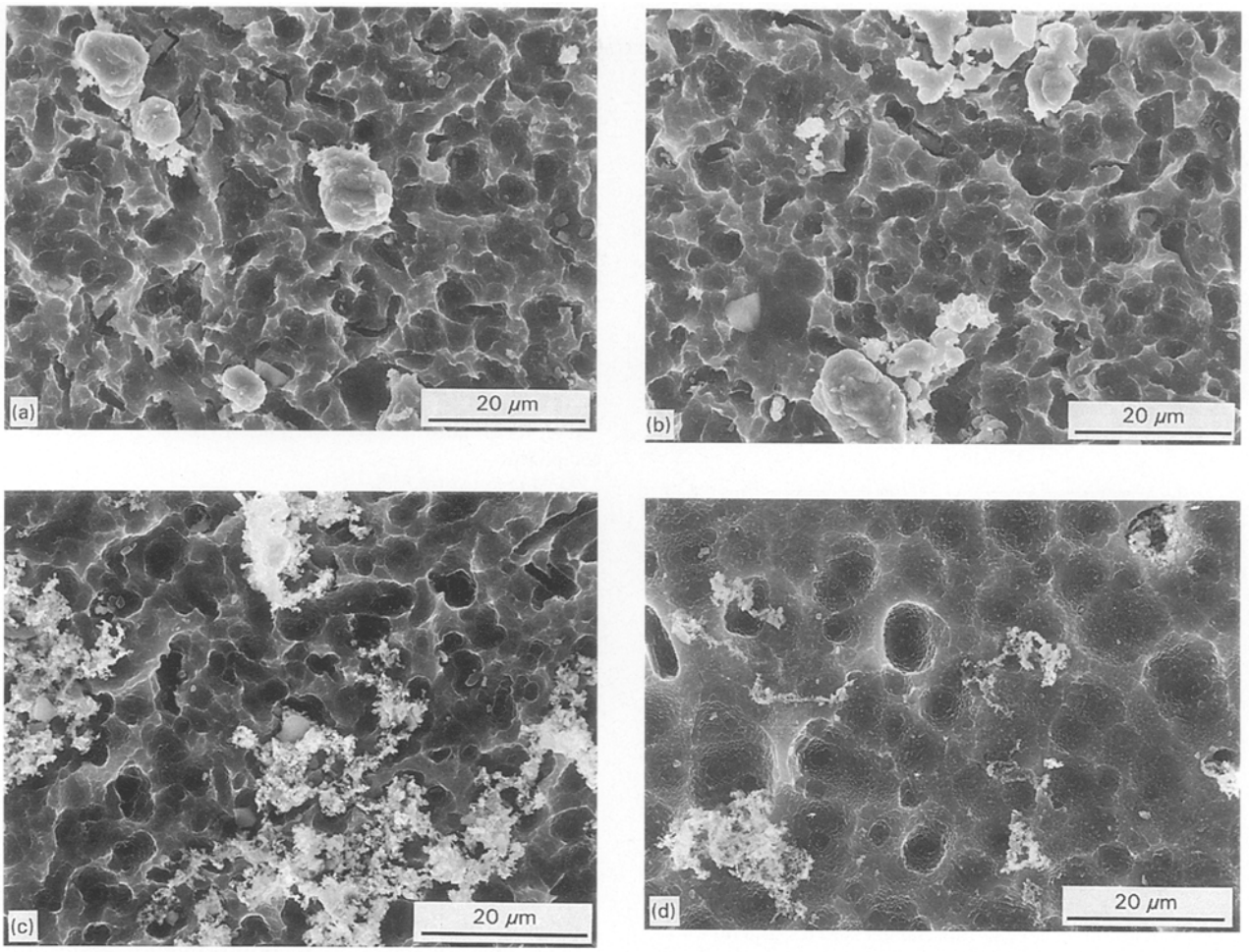

Figure 3 Scanning electron micrographs at × 1500 magnification from samples that had been ZPO coated with identical procedures but were surface conditioned differently according to temperature and subsequent water rinse or not: (a) C1, surface conditioned at 25 °C then H_2O rinse; (b) C2, surface conditioned at 25 °C no H_2O rinse; (c) C3, surface conditioned at 40 °C then water rinse; and (d) C4, surface conditioned at 40 °C no H_2O rinse.

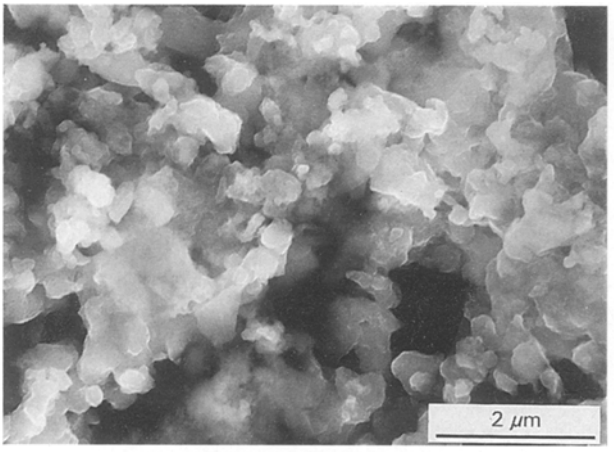

Figure 4 Scanning electron micrograph at × 15 000 from crystalline coating phase on sample C4.

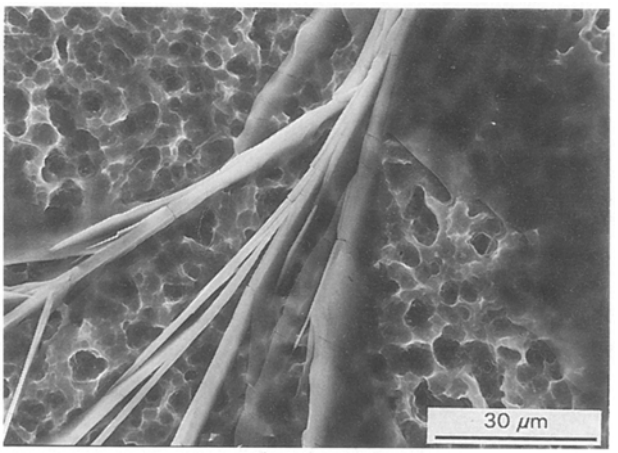

Figure 5 Scanning electron micrograph at × 1000 magnification from sample B, panel surface after Ti conditioning at 40 °C and a subsequent H_2O rinse.

observed for samples C3 and C4 that were surface conditioned at 40 °C, i.e., respectively, with and without the water rinse. The crystal grains that form the clusters are smaller (typically < 0.5 μm, see Fig. 4). Furthermore, the density of the crystal patches on sample C3 (with water rinse) appears to be higher than that of sample C4 (without the water rinse). According to the observations of morphology with SEM, sample C3 appears to have the best crystalline coating phase among the four samples (C1–C4); it not only has fine crystal grains, but also the highest coverage.

To gain insight to the role of the surface conditioning, which improves the resultant coating, the morphology of sample B, i.e. sample C3 before the coating treatment, was studied, and its SEM micrograph at × 1000 magnification is given in Fig. 5. A "porous-like" structure, that is very similar to that of the

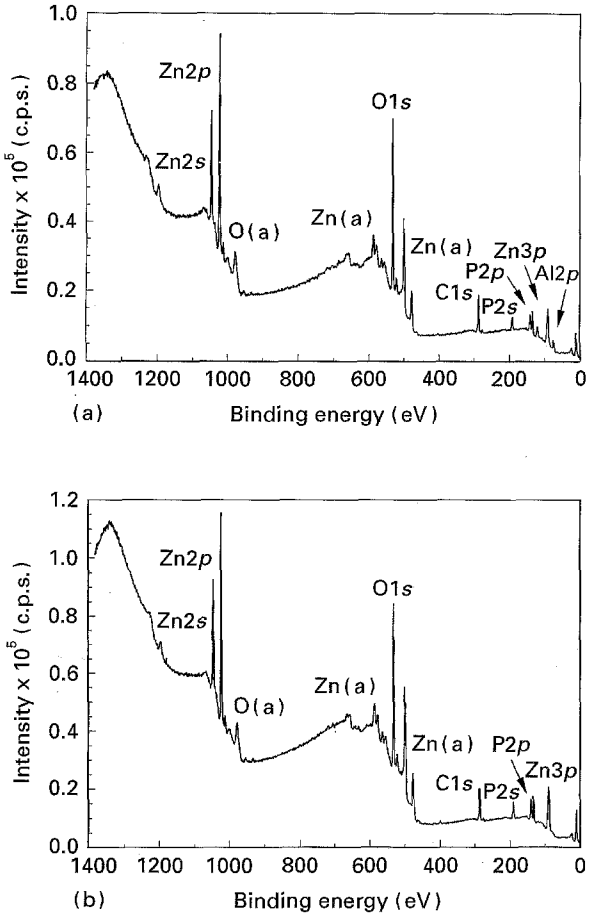

Figure 6 XPS survey spectra from samples: (a) C2, and (b) C4.

amorphous phase of the coating layer, is observed on the conditioned surfaces, but it must be emphasized that this porous-like structure results from the surface conditioning (sample B has not been subjected to the coating process). Of particular interest is the leaf-like feature, which corresponds to a membrane formed from the unremoved colloid after the water rinsing. Such a membrane is much thicker in the absence of the rinse, e.g. for sample C4, and can be observed by eye to cover the whole surface. However, direct SEM observation of these thick membranes is difficult, apparently due to charging problems. These membranes can peel off the surface after dipping into the coating bath. The effect of this membrane on the phosphating process will be discussed in the following sections.

3.2. XPS study

The study of morphology helps evaluate one aspect of a phosphate coating layer, but inevitably fuller evaluations, and an understanding of the coating chemistry involved, require information about chemical composition and chemical state. Accordingly, chemical analysis with XPS has been carried out on all the coated samples C1–C4, and in all cases XPS shows the presence of Zn, P, O and a small amount of C, regardless of the particular surface conditioning procedure.

TABLE I Relative atomic ratios[a] for six zinc phosphate coated Al samples as determined by XPS for normal exit angle. Four samples C1–C4 (Fig. 1) received Ti surface conditionings as discussed in the text, whereas the two samples C5 and C6 did not. C5 was prepared in the same ZPO coating bath, while that for C6 additionally had some fluoride as in [11]

Sample	Zn/Al	P/Al	Zn/P
C1	0.280	0.24	1.180
C2	0.760	0.87	0.880
C3	0.590	0.78	0.760
C4	[b]	[b]	0.660
C5	0.033	0.54	0.061
C6	0.240	1.04	0.230

[a] Al in these ratios refers to the total of the metallic and oxide components.
[b] No Al detected by XPS.

The Al signal, on the other hand, could be observed on C1–C3, but not on C4. Illustrative survey spectra from samples C2 and C4 are shown in Fig. 6, where it should be noted that XPS is probing the coating layer as a whole, including both the amorphous base and the crystal grains. Comparisons of the chemical compositions of the surface regions of these samples were made from measured areas for the $Zn2p_{3/2}$, P2*p* and Al2*s* peaks (as noted above), and the resulting relative atomic ratios are summarized in Table I for the coated samples. The P2*p* binding energy suggests that phosphorus exists in the form PO_4^{3-}.

The effect of the surface conditioning temperature was examined by comparing samples C2 and C4 (both no water rinse), and C1 and C3 (both rinsed with water). Table I clearly indicates that the samples that were surface conditioned at 40 °C (C3 and C4) have higher amounts of Zn and P compared to those surface conditioned at room temperature (C1 and C2). Further, the evidence in Table I indicates that samples, which are not water rinsed in the conditioning process (C2 and C4), yield higher amounts of Zn and P in the coated layer than those which are water rinsed in the surface conditioning. In general, the higher Zn and P contents, and the corresponding diminution in the Al seen by XPS, indicates greater amounts of zinc phosphate in the coating layer. The relative composition analysis therefore indicates that an elevated surface conditioning temperature, and the absence of a water rinse, are favourable factors for the formation of zinc phosphate. In fact, the XPS assessment of the coating on sample C4 shows a Zn/P ratio of 0.66, which of the coated samples considered here is the closest to the 0.88 measured from a standard sample of ZPO*.

The Ti colloid pretreatment produces a membrane that covers the surface, partially or completely depending on whether a water rinse is done or not. Fig. 7 shows an XPS survey spectrum measured from sample B, i.e. after the Ti colloid pretreatment; interestingly only a trace amount of Ti is evident, while large amounts of Al and SO_4^{2-} are detectable. The strong

* Through this paper the authors refer to phosphate as based on the PO_4^{3-} ion, but the usage should be seen as more generic since involvement by $H_2PO_4^-$ and HPO_4^{2-} ions is likely in the surface regions.

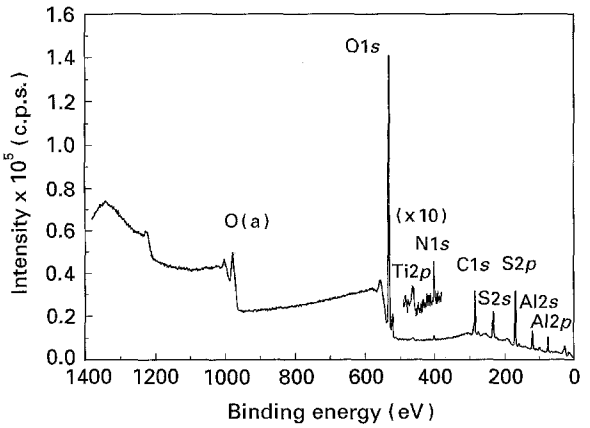

Figure 7 XPS survey spectra from sample B, panel surface after Ti conditioning at 40 °C and a subsequent H_2O rinse.

Al signal with metallic and oxide components comes mainly from the substrate, although there is believed to be some contribution from the membrane [possibly in the form of $Al_2(SO_4)_3$].

3.3. Static and imaging SIMS analysis

The SEM morphology study (Fig. 3) indicated that the coating layer consists of two phases, and the crystalline phase of sample C3 has the highest surface coverage among the four samples according to this evaluation. Chemical analysis with XPS, on the other hand, showed that sample C4 has the highest zinc phosphate content. That opens the question of the chemical composition of the two coating phases, and in particular how the morphology correlates with chemical composition. Accordingly, a SIMS study has been undertaken to probe such questions.

The non-detection by XPS of Al on C4 indicates that this element is not significantly present in either of the two coated phases on this sample, and this guides one to concentrate the SIMS investigation mainly on sample C3. In particular, static SIMS ion species surveys, and SIMS elemental mapping, have been carried out to identify the chemical composition of the coating phases. Identifiable ion species are Al^+ (mass 27) and Zn^+ (masses 64, 66, 68) in the positive SIMS spectrum, and O^- (mass 16), PO_2^- (mass 63) and PO_3^- (mass 79) in the negative spectrum. No attempt has been made yet to obtain the relative abundances of the elements in the sample, but these observations are in good accord with the XPS analysis in the previous section and the earlier study by Heung *et al.* [11]. In summary, combined analysis by XPS and static SIMS indicates that the whole coating layer corresponds to a mixed aluminium and zinc phosphate, i.e. it corresponds to a formula like $Al_xZn_yPO_4$.

Fig. 8 shows some SIMS maps for sample C3. That in Fig. 8a shows the ion induced secondary electron image, i.e. the morphology, and Fig. 8b–d show the PO_2^-, Zn^+ and Al^+ distributions on the same sampling area. A patch of crystal grains can be clearly identified in the secondary electron image (Fig. 8a) at the central region. The dimension of this patch is ~20 μm, which is consistent with the sizes of patches observed in the SEM micrograph (Fig. 3c). The darker background is identified as the amorphous base. The PO_2^-, Zn^+ and Al^+ images shown in Fig. 8b–d correlate with the secondary electron image, and in particular these ion signals are more intense on the patches of crystal grains than on the amorphous base. Possibly this difference arises from the crystalline phase having a higher yield for these ion species, but, if so, this would complicate quantitative comparisons of composition between the two coating phases. On the other hand, the clear morphological correlation between the secondary electron image and the ion maps provides unambiguous information about the chemical composition of these two coating phases. From the ion maps in Fig. 8b–d, and survey scans of areas without crystals, it is clear that both the crystal patches and the amorphous base contain zinc, aluminium and phosphate.

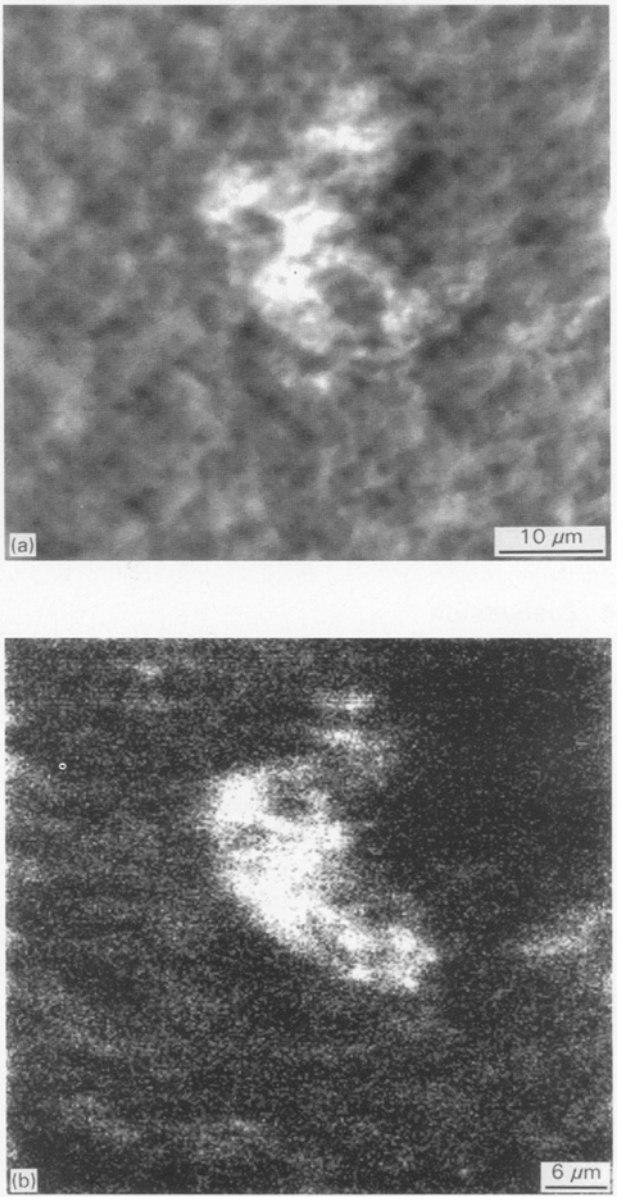

Figure 8 (a) Secondary electron image from sample C3, plus SIMS maps from the same region for (b) PO_2^-, (c) Zn^+, and (d) Al^+ images.

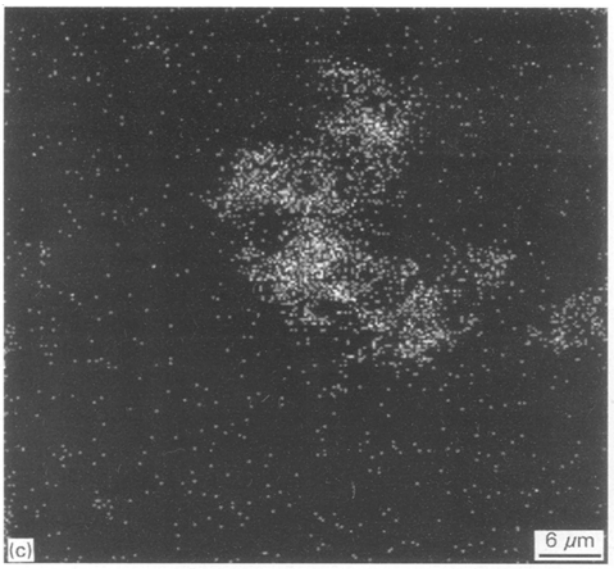

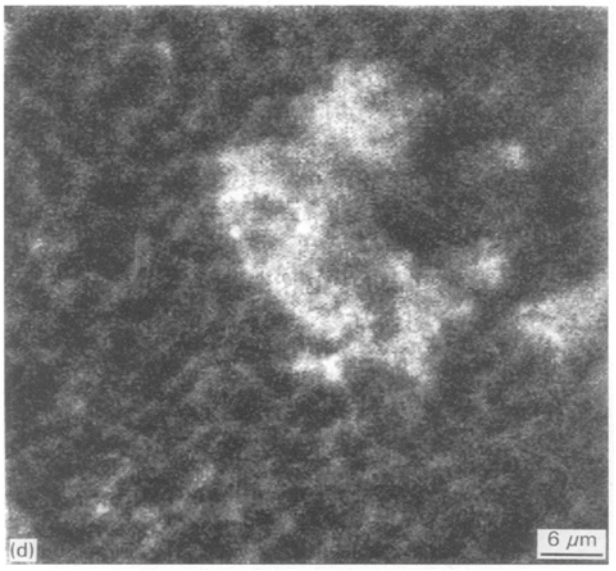

Figure 8 Continued.

4. Discussion

4.1. Effect of Ti surface conditioning on coating morphology and composition

The effect of the Ti colloid surface conditioning on the morphology of the coatings is mainly manifested in the crystalline coating phase. In particular, larger coverage and finer crystal grains, in patch form, were observed for the crystalline phases on samples C3 and C4, while only well separated coarse crystals were found on samples C1 and C2. The sizes of the crystal grains are similar for samples C1 and C2, and for samples C3 and C4. The morphologies of samples C1 and C2 are comparable to each other, and to those of coatings formed in the same coating bath but without the Ti colloid pretreatment (SEM micrograph not shown). From these comparisons, it is clear that the Ti colloid surface conditioning has the effect of reducing average grain size, and increasing coverage for the elevated surface conditioning temperature (40 °C). The coverage of the crystalline coating phase orders as C3 < C4 < C1, C2 among the four samples.

The XPS analysis indicates that the Ti colloid pretreatment significantly affects the chemical compositions of the coatings. Relative compositions for coatings formed in a similar manner [11], but without the Ti pretreatment, are also included in Table I; samples C5 and C6 are formed in the same coating bath, except C6 has a fluoride additive. The coating from the simplest treatment (C5 in Table I) has the lowest value of Zn/Al, while the fluoride additive (C6 in Table I) effects an increase in Zn content. The Ti colloid pretreated samples reported in the present work (C1–C4), on the other hand, show the highest Zn/Al ratios among the three categories, i.e. simple coating treatment, fluoride additive and Ti pretreatment. Furthermore, the use of the fluoride additive and the Ti colloid pretreatment also both appear to enhance the P/Al ratio. In general, higher Zn/Al and P/Al ratios can be taken to indicate larger amounts of zinc phosphate in the coating layer. The composition ratios listed in Table I therefore provide an indicator for evaluating the respective coatings. According to this quantitative comparison, the fluoride additive and the Ti colloid pretreatment have similar effects, with the Ti pretreatment apparently more effective in increasing the Zn and P content. A result of particular importance is the non-detection of Al, and high Zn and P contents, for sample C4. As noted above, one concludes that this coating has the closest Zn/P ratio to that seen by XPS from a standard zinc phosphate sample.

The XPS analysis provides quantitative information on the variation of relative atomic compositions among the coated samples. However, this information applies to areas sampled over a few millimetres in one-dimension. According to the SEM observation, such sampling areas would normally encompass both the amorphous and crystalline coating phases, since the amorphous phases are only partially covered by the crystalline phases on the four coating samples C1–C4. The SIMS analysis, on the other hand, has provided a correlated morphology–composition investigation for sample C3, which indicates that both the amorphous and the crystalline phases contain Zn, Al and phosphate. The focus of the imaging SIMS analysis was on crystalline patches typically of size $\sim 10 - 50$ μm (a limitation of spatial resolution does not allow imaging of the individual crystal grains for all four samples studied here). However, quantitative composition comparisons would not be easy because of the apparent different ion yields from the different phases. Despite the limitations of each individual technique, their combination can help shed new understanding. In particular, no correlation was found between the crystalline phase coverage and zinc phosphate concentration. The coverage varies among the four coated samples as C3 < C4 < C1, C2, while the amount of Zn follows C4 < C2 < C3 < C1. This emphasizes that characterizations relying exclusively on morphology analysis, or exclusively on chemical composition analysis, could be incomplete and perhaps even misleading. Accordingly, the approach of using complementary characterization techniques, as here, should help gain a more complete understanding of the nature of the coating layers.

4.2. Role of Ti surface conditioning in coating process

The $ZnO + H_3PO_4$ coating process has been discussed previously [9–11], and basically it involves competing reactions of etching and coating as depicted by

$$2\,Al + 6H^+ \rightarrow 2\,Al^{3+} + 3H_2 \quad (1)$$

$$Al^{3+} + PO_4^{3-} \rightarrow AlPO_4 \quad (2)$$

$$3Zn^{2+} + 2\,PO_4^{3-} \rightarrow Zn_3(PO_4)_2 \quad (3)$$

The consumption of H^+ in Equation 1 helps to drive the coating Equations 2 and 3, but formation of H_2 at the reaction surface may simultaneously help block the precipitation of $AlPO_4$ and $Zn_3(PO_4)_2$, i.e. the coating processes [12]. So in general there must be some balance between etching and coating, and even the latter involves two competing Equations 2 and 3. Additives and pretreatment processes can affect the balance between the various competing reactions, and such chemical manipulations have been important in the phosphating of steel [4]. On aluminium, a fluoride additive [11] helps suppress Equation 2 by forming the AlF_6^{3-} complex, which in turn facilitates the precipitation of zinc phosphate in Equation 3. The enhancement of the Zn and P content due to the Ti colloid surface conditioning observed in the present work indicates that this pretreatment has a similar function in changing the balance between Equations 2 and 3. The membrane formed from the Ti colloid pretreatment peels off after the coating process starts, and therefore it appears to play a key role in affecting the balance at the initial point. However, the details of how this membrane works, including its stronger effect when formed at 40 °C, remain unclear. The observation that membranes formed without water rinsing have a stronger effect than those with water rinsing seems to indicate the importance of the membrane coverage. A similar "retardation effect" by water rinsing has also been observed in the predip treatment in $Ti_3(PO_4)_2$ solution for steel [4].

4.3. Role of amorphous coating phase

The evidence here suggests that the amorphous coating phase has the role of physically bridging between the substrate and the crystalline coating phase. Due to the fundamental differences between aluminium and zinc phosphate, it is probably reasonable to assume that zinc phosphate crystals do not bond well on to the metal–oxide surface by direct chemical bonds. On the other hand, the amorphous phase is less restricted for matching long range order, and it seems plausible to hypothesize that the formation of an amorphous phase is a necessary first step if the crystalline phase is to be grown.

5. Conclusion

The Ti colloid surface conditioning treatment studied here appears to have a similar effect to that of adding fluoride to the coating suspension as investigated earlier [11]. The Ti surface conditioning affects both the morphology and the chemical composition of the coating layer which consists of two phases, an amorphous phase and a crystalline phase. Morphologically, this pretreatment reduces the average crystal grain size and increases the coverage of the crystalline coating phase; in terms of chemical composition, this treatment enhances the Zn and P contents in the coating layer. Different surface conditioning procedures have been evaluated by characterizing the final coating layer. In particular, surface conditioning at 40 °C, compared with room temperature, was shown to increase the amounts of Zn and P in the coatings; by contrast, these contents were decreased by giving the Ti conditioned surface a water rinse prior to the coating treatment. The Ti colloidal membrane formed on the conditioned surface clearly plays a key role in the coating chemistry, although the determination of mechanistic details of this pretreatment remains a subject for future study.

Acknowledgements

We acknowledge support for this research provided by the Defence Research Establishment Pacific and by the Natural Sciences and Engineering Research Council of Canada.

References

1. T. FOSTER, G. N. BLENKINSOP, P. BLATTLER and M. SZANDOROWSKI, *J. Coating Technol.* **63** (1991) 91.
2. *Idem, ibid.* **63** (1991) 101.
3. G. ADRIAN and A. BITTNER, *ibid.* **58** (1986) 59.
4. W. RAUSCH, "The Phosphating of Metals" (Finishing Publications, Teddington, 1990) Ch. 3.
5. D. B. FREEMAN, "Phosphating and Metal Pre-treatment" (Industrial Press, New York, 1986) Ch. 8.
6. T. W. CAPE, "Metals Handbook", Vol. 13 Corrosion (American Society for Metals International, Metals Park, OH, 1987) p. 383.
7. A. TURUNO, K. TOYOSE and H. FUJIMOTO, *Kobelco Tech. Rev.* **11** (1991) 14.
8. K. TOYOSE, A. TSURUNO, H. FUJIMOTO and S. KOGA, *ibid.* **13** (1992) 56.
9. W. F. HEUNG, Y. P. YANG, P. C. WONG, K. A. R. MITCHELL and T. FOSTER, *J. Mater. Sci.* **29** (1994) 1368.
10. W. F. HEUNG, Y. P. YANG, M. Y. ZHOU, P. C. WONG, K. A. R. MITCHELL and T. FOSTER, *ibid.* **29** (1994) 3653.
11. W. F. HEUNG, P. C. WONG, K. A. R. MITCHELL and T. FOSTER, *ibid.* (1995) in press.

Received 17 March 1995
and accepted 17 July 1995